Intensity Modulation of Transmitted Light at the Ground-State Hyperfine Frequency of K^{39}†

ARTHUR H. FIRESTER* AND THOMAS R. CARVER
Palmer Physical Laboratory, Princeton University, Princeton, New Jersey
(Received 18 April 1967)

This paper discusses intensity modulation of transmitted light at 462 MHz due to coherence between sublevels of the K^{39} ground state. A concise theory of transmitted-light modulation is presented, using the density-matrix and monitoring-operator formalism. The theory and construction of an ultrahigh-frequency photodetection system is described. The auxiliary apparatus is also described, together with experimental conditions under which signals have been observed. It is suggested that a possible application of this technique is a wide-range magnetometer.

INTRODUCTION

THE development of the optical pumping of atoms has led to the creation of a new branch of radio-frequency spectroscopy and has extended the optical methods for studying matter. One new technique, the modulation of light transmitted by an optically pumped atomic sample, was first experimentally reported by Bell and Bloom,[1] following Dehmelt's[2] publication of a phenomenological theory of the effect. The subsequent work of Dodd and Series[3] and Barrat[4] developed a quantum-mechanical theory and extended the experimental techniques to the modulation of scattered radiation.

Low-frequency Zeeman light modulation is readily observable, but previous attempts to observe the very-high-frequency light modulations characteristic of the ground-state hyperfine splittings of the alkalis have not been successful. This appears to have been the consequence of an incomplete understanding of light-beat theory or a lack of a suitable high-frequency photodetector. In this paper, we will discuss the theory and construction of a high-frequency narrow-band photodetector, the necessary associated detection system, and a general quantum-mechanical light-beat theory derived from perturbation theory. Other published light-beat theories are either classical,[1,2] deal with light beats in scattered radiation,[3,4] or are not readily accessible.[5] Previous theories have confined themselves to light beats between Zeeman or hyperfine sublevels having the same total angular momentum.[6] In this work these theories are not quite applicable. The light-beat theory presented here will consider a general coherence-producing perturbation, will delineate the region of applicability of the monitoring-operator[7] approach, and will more rapidly arrive at an expression for the modulation of the light absorption than previous theories.

The principle underlying light-beat phenomena is quite basic. If two or more atomic levels are coherent or phase related throughout a bulk sample, there may appear an interference term in the electric-dipole absorption or emission probability. This term oscillates with the same periodicity as the source of coherence and shows a resonant behavior at the frequency separation of the atomic levels. Rather than restrict ourselves to only those cases where the generation of the coherence is exactly soluble, we will consider a general perturbation theory and determine an approximate solution.

A level diagram of the ground and first excited states of potassium 39 is illustrated in Fig. 1. The electronic ground state is a $^2S_{1/2}$, which, because of a nuclear spin of $\frac{3}{2}$, is split into two hyperfine levels. They are characterized by total angular momentum F, of value 2 and 1, and, in zero magnetic field, are separated by 459.72 MHz.[8] In a weak magnetic field, the $F=2$ level splits into five sublevels and the $F=1$ into three. The relative absorption probabilities of σ^+ light, which connects the ground and first excited states, are indicated by the numbers above the lines corresponding to each of the sublevels.

THEORY

Rather than deal with the actual atomic system, we will consider a simplified quantum-mechanical system having only two "ground states" and a single "excited state." The system is subject to the effects of a time-dependent perturbation which connects the ground states, and is irradiated by a light source which approximately connects the ground and excited states. In practice, this light source simultaneously performs two functions. As a relaxation process, it acts to generate a non-Boltzmann population difference in the

† Research supported by a grant from the National Science Foundation.
* Present address: RCA Laboratories, Princeton, New Jersey.
[1] W. E. Bell and A. L. Bloom, Phys. Rev. **107**, 1559 (1957).
[2] H. G. Dehmelt, Phys. Rev. **105**, 1924 (1957).
[3] J. N. Dodd and G. W. Series, Proc. Proc. Roy. Soc. (London) **A263**, 353 (1961).
[4] J. P. Barrat, Proc. Roy. Soc. (London) **A263**, 371 (1961).
[5] C. Cohen-Tannoudji, J. Phys. (Paris) **7**, 423 (1962).
[6] T. McIlrath, thesis, Princeton University, 1966 (unpublished). As far as the authors know this is the only complete quantum-mechanical theory of absorption light beats in English.
[7] T. R. Carver and R. B. Partridge, Am. J. Phys. **34**, 339 (1966).
[8] N. F. Ramsey, *Molecular Beams* (Oxford University Press, London, 1956), Chap. IX, p. 255.

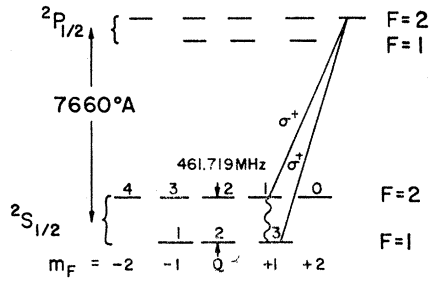

FIG. 1. Energy-level diagram, showing the ground and first excited state of K^{39}. The ground-state hyperfine splitting is 461.719 MHz in zero field.

ground state. This is because the various sublevels have quite different absorption probabilities[9] (Fig. 1). As a means of detection, the transmitted intensity of the light beam changes. We will devote our attention only to this latter function.

This simplified system is characterized by a Hamiltonian H, which can be subdivided as follows:

$$H=H_0+R+V. \tag{1}$$

The two terms R and V are considered to be small perturbations. R includes the effects of the light, whereas V represents the coherence producing perturbation; e.g., an rf magnetic field. H_0 is the Hamiltonian of the atomic system in the absence of both the coherent perturbation and the optical perturbation. The excited-state eigenstate of H_0 is denoted by $|e\rangle$, and the ground-state eigenstates are denoted by $|m\rangle$, $|n\rangle$. Their energies are $\hbar\omega_e$, $\hbar\omega_m$, and $\hbar\omega_n$, respectively.

The light absorbed, L_{AE}, is equal to the time rate of change of the ensemble excited-state population (ignoring excited-state relaxation to the ground state). That is,

$$L_{AE}=\langle e|\dot{\rho}_E|e\rangle, \tag{2}$$

where ρ_E is the ensemble density matrix. It is convenient to consider the problem in the interaction representation. An operator A transforms to an operator in the interaction representation, A^I, according to the rule[10]

$$A^I=\exp(iH_0t/\hbar)A\exp(-iH_0t/\hbar). \tag{3}$$

The light absorbed by a single atom is

$$L_A=\langle e|\dot{\rho}^I|e\rangle, \tag{4}$$

where ρ^I is the atomic density matrix in the interaction representation.

The equation of motion of the density matrix in the interaction representation is

$$i\hbar\dot{\rho}^I=[R^I+V^I,\rho^I]. \tag{5}$$

An iterative solution to Eq. (5) is substituted into Eq. (4). Later, when we average the light absorption over the ensemble of incoherent light sources which represent a real lamp, it will be seen that the ensemble average of R^I is zero. Thus, all terms which are first order in the optical perturbation can be neglected. To second order, terms which are quadratic in V^I are zero, since V^I does not connect the ground state with the excited state. The result, to the lowest nonvanishing order, is

$$L_A(t)\approx(1/i\hbar)^2 \times\langle e|\left[R^I(t'),\int_{t_0}^{t}[R^I(t'),\sigma^I(t')]dt'\right]|e\rangle, \tag{6}$$

where $\sigma^I(t')$ is the density matrix which would describe the system in the absence of the optical perturbation at time t', and where t_0 is the time at which the optical perturbation is turned on.

At this point, it is convenient to transform Eq. (6) back to the Schrödinger representation. The result is

$$L_A(t)\approx(1/\hbar)^2\sum_{m,n}\int_{t_0}^{t}[R_{em}(t)R_{ne}(t')\exp\{i\omega_{em}(t-t')\} +R_{em}(t')R_{ne}(t)\exp\{-i\omega_{en}(t-t')\}]\sigma_{mn}(t')dt', \tag{7}$$

where $\omega_{em}=\omega_e-\omega_m$ and $\omega_{en}=\omega_e-\omega_n$.

Let us determine the form of the terms $R_{em}(t)R_{ne}(t')$. The Hamiltonian describing the interaction of an electromagnetic wave with an electron is $R=(e/m)\mathbf{A}(t)\cdot\mathbf{p}$, where $\mathbf{A}(t)$ is the vector potential of the electromagnetic field in the transverse gauge, and where $\mathbf{p}$ is the momentum of the electron. Following standard techniques,[10] we make the dipole approximation. Denote by H_s that part of H_0 which contains only the central Coulomb interaction and the kinetic energy of the valence electron, and no fine, hyperfine, or rf interactions. We may then use the commutation relations of this skeletal Hamiltonian H_s, with the position vector $\mathbf{r}$, to simplify the optical perturbation. We replace $\mathbf{p}$ by $(m/\hbar)[\mathbf{r},H_s]$. Thus, we can represent $R_{em}(t)R_{ne}(t')$ by

$$R_{em}(t)R_{ne}(t')=W^2\langle n|\hat{e}\cdot q\mathbf{r}|e\rangle\langle e|\hat{e}^*\cdot q\mathbf{r}|m\rangle A^*(t)A(t'), \tag{8}$$

where $\hat{e}$ is a unit vector in the direction of the electric field and W is the frequency separation of the ground and excited states of an atom with this skeletal Hamiltonian.

This can be simplified further by introducing the monitoring operator M_{nm} defined by Carver and Partridge[7]:

$$R_{em}(t)R_{ne}(t')=W^2M_{nm}A^*(t)A(t'). \tag{9}$$

It should be noted that the monitoring operator contains only the symmetry terms of the expression.

At this point, the problem is reduced to the determination of terms of the form $A^*(t)A(t')$. The vector potential $A(t)$ is a random operator and, as such, cannot represent a physically observed quantity. The

[9] W. Franzen and A. G. Emslie, Phys. Rev. **108**, 1453 (1957).
[10] E. Merzbacher, *Quantum Mechanics* (John Wiley & Sons, Inc., New York, 1961).

observable behavior of the system is described by an operator which is the ensemble average of the random operators. The observable quantity will be the average $\langle\langle A^*(t)A(t')\rangle\rangle_{\text{av}}$, taken over the statistical ensemble. The ensemble is stationary. Thus, the above quantity will depend only on the time difference $(t-t')$. The electric field is equal to the derivative with respect to time of the vector potential. By manipulation of Fourier transforms and by performing the ensemble average (denoted by double angular parentheses) over all the random vector potentials, we obtain the expression

$$\langle\langle A^*(t)A(t')\rangle\rangle_{\text{av}}=\int_{-\infty}^{\infty}[J(\nu)/\nu^2]\exp\{i\nu(t-t')\}d\nu, \quad (10)$$

where $J(\nu)$ is the energy per unit frequency interval of the light.[11] Thus,

$$L_A(t)=(W/\hbar)^2\sum_{m,n}\int_{t_0}^{t}dt'\int_{-\infty}^{\infty}[J(\nu)/\nu^2]\times[\exp\{i(\omega_{em}-\nu)(t-t')\}+\exp\{-i(\omega_{en}-\nu)(t-t')\}]d\nu. \quad (11)$$

Assuming a Gaussian line shape for $J(\nu)$,

$$J(\nu)=I_0\exp\{-a^2(\nu-\nu_0)^2\}, \quad (12)$$

$$L_A(t)\approx(W^2I_0\pi^{1/2}/\nu_0^2\hbar^2a)\times\sum_{m,n}M_{nm}\int_0^{t-t_0}d\tau\,\sigma_{mn}(t-\tau)\exp\{-\tau^2/4a^2\}\times[\exp\{i(\omega_{em}-\nu_0)\tau\}+\exp\{-i(\omega_{en}-\nu_0)\tau\}]. \quad (13)$$

We can replace the upper limit in the integral by infinity. This corresponds to turning on the light at an arbitrarily distant time in the past.

$L_A(t)$ is the light absorbed by a single atom. The final step is to consider the average of this quantity over the bulk sample. This is equivalent to replacing $\sigma_{mn}(t-\tau)$ by its bulk average, denoted $\langle\sigma_{mn}(t-\tau)\rangle_{\text{av}}$.

The final result for the light absorption is then

$$L_{AE}(t)=(W^2I_0\pi^{1/2}/\nu_0^2\hbar^2a)\times\sum_{m,n}\int_0^{\infty}d\tau\langle\sigma_{mn}(t-\tau)\rangle_{\text{av}}\exp\{-\tau^2/4a^2\}\times[\exp\{i(\omega_{em}-\nu_0)\tau\}+\exp\{-i(\omega_{en}-\nu_0)\tau\}]. \quad (14)$$

In our experiment the light source is broad compared with ω_{mn}. Thus, the integral is appreciably different from zero only about $\tau\approx0$. In this case, Eq. (14) reduces to the usual monitoring-operator equation,

$$L(t)\propto\sum_{m,n}M_{nm}\langle\sigma_{mn}(t)\rangle_{\text{av}}. \quad (15)$$

When the light source is narrow, compared with the separation of the coherent ground states, it becomes necessary to include the effects of the finite lifetime of the excited state. This can be phenomenologically introduced by including within the integral in Eq. (14) the term $\exp\{-\tau/\tau_e\}$, where τ_e is the lifetime of the excited state. When τ_e is short compared with the periodicity of the Hamiltonian which generates the coherence, the light absorption again reduces to Eq. (15).

In many cases, the density matrix of the atomic ensemble under the influence of H_0 and V can be solved exactly.[12] Equation (14) is not restricted to only those cases, however.

Consider a general quantum-mechanical two-state system described by a Hamiltonian

$$H=H_0+V, \quad (16)$$

where

$$V=\hbar f\exp\{-i\omega t\}+\hbar f^{\dagger}\exp\{i\omega t\}. \quad (17)$$

H_0 is the unperturbed Hamiltonian and f is a time-independent operator. We include the effects of relaxation and damping by assuming the uniform decay of all the elements of the density matrix to a uniform distribution at a rate Γ. The effects of a population regeneration are included by assuming that representative systems in the atomic ensemble are being steadily pumped into a constant configuration σ_0 at a rate W_p.[7] Assuming

$$\sigma_0=\begin{pmatrix}1&0\\0&0\end{pmatrix},$$

an approximate expression for the steady-state ensemble density matrix, expressed in terms of the eigenstates of

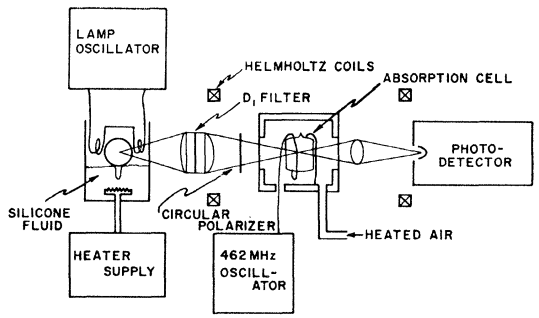

FIG. 2. Schematic diagram of the optical pumping apparatus.

[11] For details of this procedure see M. Born and E. Wolf, *Principles of Optics* (Pergamon Press, Inc., New York, 1959), Chap. 10, pp. 490–502.

[12] H. Salwen, Phys. Rev. **99**, 1274 (1955).

H_0, is easily found to be

$$\langle\sigma(t)\rangle_{\rm av}=\left(\frac{W_p}{\Gamma}\right)\begin{pmatrix}1-2|f_{mn}|^2/\Delta^2 & \exp\{i\omega t\}\ f_{mn}^*(\epsilon+i\Gamma)/\Delta^2\\ \exp\{-i\omega t\}\ f_{mn}(\epsilon-i\Gamma)/\Delta^2 & 2|f_{mn}|^2/\Delta^2\end{pmatrix}, \tag{18}$$

where $\epsilon=(\omega_{mn}-\omega)$ and $\Delta^2=\epsilon^2+\Gamma^2+4|f_{mn}|^2$.

The line shape of light-beat signals that would result from the above solution and a 2×2 Hermitian monitoring operator having nonzero off-diagonal elements depends upon the phase of the detected signal with respect to the phase of V. The two independent line shapes are

$$L_{\text{in phase}}\propto(\epsilon/\Delta^2)\cos(\omega t), \tag{19}$$

and

$$L_{\text{quadrature}}\propto(\Gamma/\Delta^2)\sin(\omega t). \tag{20}$$

APPARATUS

The apparatus necessary for the optical pumping of potassium is schematically indicated in Fig. 2. A uniform magnetic field is generated by a set of mutually orthogonal square Helmholtz coil pairs.[13] The source of the potassium pumping light is an electrodeless rf discharge lamp. The lamp is a 2-cm sphere of Corning 7070 glass. Although this glass does not have the remarkable resistance to alkali discoloration that special proprietary glasses[14] have, it is considerably more convenient than the use of alkali-resistant coatings applied to other glasses,[15] and is distinctly superior to ordinary Pyrex glass. This glass has been in use in this laboratory with notable success in the construction of sodium lamps for many years.[16] The sphere is filled with about 2 Torr of argon buffer gas. Purified potassium metal is distilled in and allowed to condense in the pull-off. When the lamp is in operation, the pull-off containing the potassium metal is immersed in a heated bath of silicone fluid at a temperature of 130°C. This temperature was experimentally determined to optimize the optical-pumping signals. In this mode of operation, the lamp output was stable to within a few percent.

The potassium D_2 line at 7699 Å is removed by a multilayer interference filter.[17] After passing through a commercial circular polarizer,[18] the light is incident upon an absorption cell containing potassium metal and a few centimeters of helium buffer gas. This cell is contained within an oven at 60°C. The oven, illustrated in Fig. 3, also serves as a shielded enclosure for a loop tuned to 462 MHz and oriented to generate an axial magnetic field. It is within this loop that the absorption cell is set. To minimize the fringing fields, the loop is a single turn of 1.5-in. wide copper strip. This strip is bent to form a "U." The loop is tuned by means of a movable wedge-shaped piece of Teflon located between the open ends of the "U," and is inductively coupled and matched to a 50-Ω source. The light transmitted through the absorption cell is then focused upon a photodetector, described in detail in the following section.

In these investigations, it was necessary to construct a high-frequency photodetector because commercial photodetectors were unsuitable. Commercial photodetectors, incorporating $S-1$ and other standard photoemissive materials (as well as photoconductive semiconductors), have been developed with a frequency response extending into the gigahertz region. Unfortunately, they also have photosensitive areas of about 0.03 cm^2 [19] (while the sensitive area of typical photoconductive semiconductor detectors is 0.002 cm^2 [20]), and are thus unsuitable for use with light sources other than lasers. In these experiments, a photosensitive area of at least 0.1 cm^2 is necessary. Since this area is small when compared with λ^2 (where $\lambda\approx66$ cm for the frequency of interest, 462 MHz), one anticipates

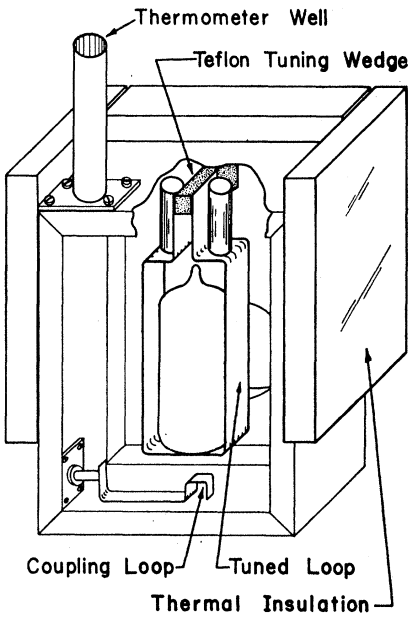

FIG. 3. Detailed diagram of the combined absorption-cell oven and tuned loop enclosure.

[13] A. H. Firester, Rev. Sci. Instr. **37**, 1264 (1966).
[14] Osram.
[15] F. X. Powell, O. Fletcher, and E. R. Lippincott, Rev. Sci. Instr. **34**, 36 (1963).
[16] G. Ruff, thesis, Princeton University, 1966 (unpublished).
[17] Spectrolab, Inc., type 8558.
[18] Polaroid, HNCP 37.
[19] R. Targ, D. E. Caddes, and B. J. McMurtry, IEEE Trans. Electron Devices **ED-11**, 164 (1963).
[20] H. P. Associates.

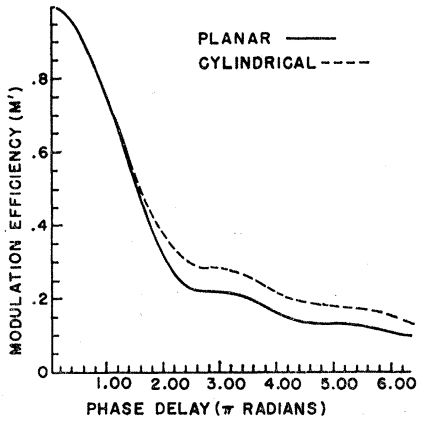

FIG. 4. Modulation efficiency for a cylindrical and planar photodiode with a 1-cm interelectrode spacing.

no difficulties due to the size of the photoemissive surface.

The problems encountered in the design of a high-frequency photodetector can be divided into three groups: (1) transit-time spread, (2) transit time, and (3) the coupling of the external circuitry in the photodiode structure. If different photoelectrons have varying transit times in crossing the diode gap, the performance of the photodetector degenerates. This transit time spread is minimized by choosing a proper geometry, and by increasing the gap potential so that the initial spread in electron energies is negligible when compared with this potential.

The effect of the finite transit time can be seen from the following discussion. As a model, consider the photodiode as a planar structure—a plane photoemissive surface separated by a distance d from a parallel plane anode, whose potential is V volts with respect to the photoemissive surface. Assuming that variations parallel to the end planes of the gap are negligible, the equation of continuity can be written

$$(\partial/\partial x)[i(x,t)/A]+(\partial/\partial t)\rho(x,t)=0, \qquad (21)$$

where $i(x,t)$ is the current for the entire area of the gap A.

Combining Eq. (21) with the divergence relation for the electric displacement,

$$(\partial/\partial x)[i(x,t)+A(\partial/\partial t)E(x,t)]=0. \qquad (22)$$

The quantity in brackets is the total current. Integrating this equation across the gap, the total current in the gap $I(t)$ is found to be

$$I(t)=i(t)-C(dV/dt), \qquad (23)$$

where C is the gap capacitance, V is the gap voltage, and

$$i(t)=\frac{1}{d}\int_0^d i(x,t)dx. \qquad (24)$$

Thus, one can treat the photodiode as a current source $i(t)$ shunted by a capacitance C.

In order to evaluate the integral in Eq. (24), it is necessary to determine the current $i(x,t)$. This is the current at time t and a plane a distance x from the photoemissive surface. It is the current which was at the photoemissive surface at time $t-\Delta t$, where Δt is the time it takes for an electron to traverse the space from the photoemissive surface to the point x. Assume that the uniform dc field across the gap is very much greater than any ac fields present, and consequently, that the ac fields have negligible influence on Δt. If we represent the ac component of the current at the photoemissive surface by $i_0\exp\{i\omega t\}$, then the driving current $i(t)$ can be written

$$i(t)=M'i_0\exp\{i(\omega t-\varphi)\}, \qquad (25)$$

where

$$M'=(2/\Gamma^2)(2+\Gamma-2\Gamma\sin\Gamma-2\cos\Gamma)^{1/2} \qquad (26)$$

and

$$\varphi=\arctan[(\Gamma\cos\Gamma-\sin\Gamma)/(1-\cos\Gamma-\Gamma\sin\Gamma)]. \qquad (27)$$

The gap transit angle Γ is defined as $\Gamma=\omega d(2m/Ve)^{1/2}$, where e and m are the electronic charge and mass, respectively.

Figures 4 and 5 are graphs of the modulation efficiency M' and phase angle φ versus the transit angle Γ. (It should be noted that M' is quite distinct from the modulation efficiency of an electron "drifting" across a gap.)

Instead of a planar photodiode, a diode having a cylindrical structure (a type 917 photocell) was actually used. After the completion of the experimental work, it was suggested[21] that the cylindrical geometry is considerably poorer than the planar one. This suggestion was pursued further and the effects of the changed geometry were calculated. The calculations are not physically interesting and only the results will be given.

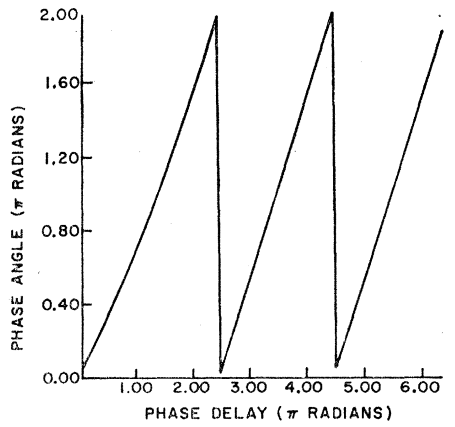

FIG. 5. Phase of effective current for a planar photodiode.

[21] Keith Jefferts (private communication).

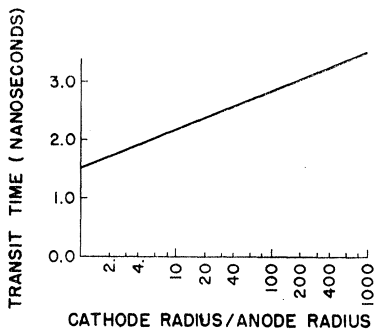

FIG. 6. Electron transit time versus cathode/anode radius for a cylindrical photodiode; (cathode radius)—(anode radius) = 1 cm. Potential difference = 500 V.

The case of the planar diode is more instructive and still applicable to a great extent.

The electron transit time for an axially symmetric cylindrical diode depends on the ratio of the radii of the electrodes, as well as on the interelectrode separation and potential difference. For a fixed spacing and potential difference, the transit time decreases as the radii are increased and approaches the transit time of a planar structure with the same interelectrode spacing and potential difference. This is illustrated in Fig. 6, which is a plot of transit time versus the ratio of outer-electrode radius to inner-electrode radius for a 1-cm interelectrode spacing and a 500-V interelectrode potential difference.

The modulation efficiency M', for the various cylindrical structures covered by Fig. 6 is not appreciably different from the modulation efficiency of a planar structure.

As has been previously shown, a reasonable model of a photodiode is a current generator $i(t)$ shunted by a capacitance. Maximum power output is obtained when the load is a very high Q inductor which resonates with the capacitance at the frequency of interest. At a frequency of 462 MHz, a shorted TEM transmission line, slightly less than a quarter wavelength long, is a high Q inductor. However, there are some conflicting design choices. One would like the capacitance per unit length of the line to be high, so that the lumped capacitance of the photodiode is not an appreciable fraction of the total capacitance of the shorted line. However, if the line is considerably larger than the photodiode, a sharp impedance discontinuity will exist between the line and the photodiode. The assumption that one is capacitively foreshortening the line is no longer a valid approximation. The actual construction, illustrated in Fig. 7, is a compromise of the various parameter choices. A type-917 photodiode with its base removed, is connected to a shorted transmission line which has been folded in half to keep the total length down. The cross section of the line is similar to "stripline."[22]

The metal tube through which the light enters the photodetector serves to prevent rf radiation from leaving or entering the internal cavity. Its diameter is 5 cm and its length is about 15 cm. Thus, it acts as a waveguide beyond cutoff for 462 MHz and yields an attenuation of about 80 dB. A tap near the shorted end of the transmission line acts as an autotransformer to match the photodetector to a 50-Ω line. The measured Q of the structure is about 150. Assuming a lumped circuit model, the equivalent load resistance of the current source $i(t)$ is about 25 kΩ.

Throughout this investigation it was of major concern to be certain that spurious interference and noise would neither be mistaken for real signals nor overshadow these signals. A form of a homodyne-phase-sensitive detection system,[23] illustrated in Fig. 8, satisfies these requirements. The photodetector current is amplified by a four-stage stagger-tuned grounded-base transistor amplifier. This amplifier has a power gain of about 50 dB and a bandwidth of 3.5 MHz centered at 462 MHz. The amplifier output is fed into the signal port of a four-diode ring modulator.[24] A 7-dBm reference, which is derived from the same rf oscillator that drives the tuned loop about the absorption cell, is fed into a reference port. The phase of the reference relative to the photodetector signal can be varied by means of a stretchable line connecting the rf oscillator with the tuned loop. The third port of the ring modulator is the output.

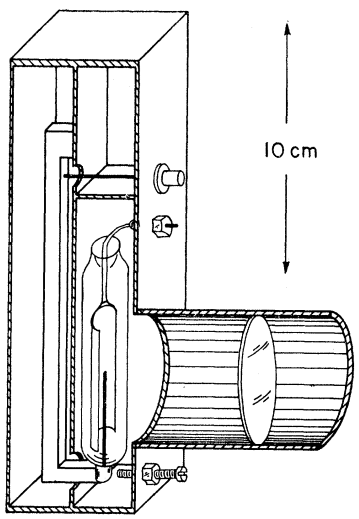

FIG. 7. Diagram of ultra-high-frequency photodetector.

[22] G. L. Matthaei, L. Young, and E. M. T. Jones, *Microwave Filters, Impedance-Matching Networks, and Coupling Structures* (McGraw-Hill Book Company, Inc., New York, 1964), Chap. 5, pp. 168–196.

[23] J. R. Kerr, IEEE Trans. **IM-14**, 209 (1965).

[24] Hewlett-Packard, 10514A Mixer.

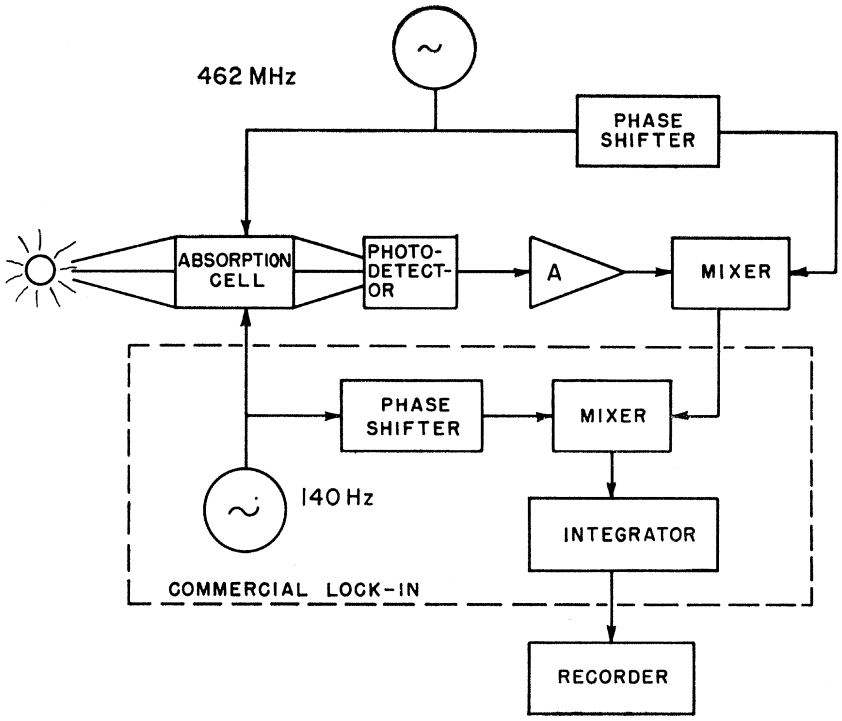

FIG. 8. Block diagram of photodetection system.

To discriminate between a light-modulation signal and rf leakage, the magnetic field at the absorption cell is modulated a few mG at 140 Hz. This field modulation generates 140-Hz sidebands on the 462-MHz light modulation but leaves the rf leakage unaffected. The output of the ring modulator is fed into a commercial lock-in amplifier whose reference is the magnetic field modulation. The resulting system of amplifier, ring modulator, and commercial lock-in has a bandwidth determined by the integration time of the commercial lock-in. In practice, the integration time was set at 10 sec.

RESULTS

Both the symmetric and asymmetric light-beat signals, due to coherence between the $F=2$, $m_F=1$ and $F=1$, $m_F=1$ ground-state hyperfine sublevels of potassium have been observed.[25] These observations were made using a monitoring light beam consisting of σ^+ polarization, which was directed along the axis of the rf and steady-state magnetic fields. Under these circumstances one expects to see light beats only between the $F=2$, $m_F=1$ and $F=1$, $m_F=1$ states. Figure 9 is a tracing of the high-frequency and zero-frequency signals versus magnetic field. The lower trace is that of the zero-frequency detection system. The left-hand resonance is due to the $\Delta m_F=0$ ($F=2$, $m_F=1$ to $F=1$, $m_F=1$) transition, while the right-hand resonance is due to the $\Delta m_F=1$ ($F=2$, $m_F=2$ to $F=1$, $m_F=1$) transition. The $\Delta m_F=1$ transition is caused by the fringing fields of the rf loop. If an rf field perpendicular to the steady-state magnetic-field axis had been used, the $\Delta m_F=1$ zero-frequency resonance would have been many times larger than the $\Delta m_F=0$ resonance. Careful design and orientation of the tuned rf loop eliminated most of the nonaxial fields. The high-frequency signal, the upper trace in Fig. 8, shows a resonance between the $F=2$, $m_F=1$ and $F=1$, $m_F=1$ sublevels. It is an approximate derivative of the asymmetric line shape. This differentiation is a consequence of the lock-in detection system. It is evident (Fig. 1) that the $F=2$, $m_F=2$ and $F=1$, $m_F=1$ sub-

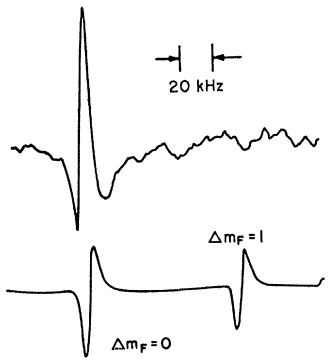

FIG. 9. The upper trace is the output of the 462-MHz light-beat detection system. An asymmetric line shape is shown. The lower trace is the output of the zero-frequency detection system.

[25] A. H. Firester and T. R. Carver, Phys. Rev. Letters **17**, 947 (1966).

levels are not coupled by light to an excited state, and thus there is no light-beat resonance corresponding to this transition on the upper trace in Fig. 9.

The symmetric line shape of the $\Delta m_F=0$ transition has also been observed. The phase of the reference applied to the ring modulator is shifted 90° from that position at which the asymmetric line shape is maximized. Then the rf power applied to the absorption cell is reduced. [It can be seen from Eqs. (19) and (20) that the optimum rf power for the asymmetric signal is larger than the optimum power for the symmetric signal.] Having made these adjustments, the symmetric line shape is easily observed.

As a check on the theory of light beats, the $\Delta m_F=0$ transition was also observed using a monitoring light beam of σ^- radiation. This was done by changing the polarization of the light beam so that it was no longer pure σ^+, but rather an admixture of σ^+ and σ^-. A σ^- polarizer was then placed just in front of the photodetector to prevent the detection of modulation of the σ^+ light. The signal-to-noise ratio of this signal was considerably poorer than that of the previous signals. One effect of the change in pumping beam polarization from pure σ^+ to an admixture of σ^+ and σ^- is that the population difference between the (2,1) and (1,1) ground states is reduced. Monitoring-operator theory predicts that the phase of the signal observed using σ^- radiation differs by 180° from that observed using σ^+ radiation. This was experimentally verified.

As a further verification of the theory, the $\Delta m_F=1$ transition was observed by using a monitoring beam consisting of σ^+ and π radiation. This is obtained by rotating the steady-state magnetic field so that the light beam and the rf magnetic field are no longer parallel to the steady magnetic field. Thus, if the steady magnetic field defines the axis of quantization, the rf magnetic field now has an off-axis component and the light beam is an admixture of σ^+, σ^-, and π radiation. This signal is quite easily observed, since the population difference between the (2,2) and (1,1) levels can be made quite large.

CONCLUSIONS

The previously developed light-beat theory clearly shows the derivation of the monitoring-operator formalism. The monitoring operator contains all the symmetries of the ground and excited states. The effects of the spectral distribution of the light source are contained within the integral in Eq. (14). Light beats, like other quantum-mechanical interference effects, are only observable when the alternative routes to the excited state are in principle not distinguishable. This is the case when the light source is broad. If the light source is narrow, the lifetime of the excited state must be short compared with the period of the light beat if the light beats are to be observed. (It should be noted that this theory cannot be directly applied to the case of excitation by a laser. The high light intensity precludes the assumption that the light is a small perturbation.)

A possible application of this work is the construction of a self-oscillating light-beat magnetometer[26] using hyperfine light modulation. The light-beat signal is amplified and fed back to drive the tuned loop. Field changes as large as 20 G would require frequency excursions of about 14 MHz. This is small compared with the zero-field frequency of 460 MHz. Thus, the percentage bandwidth would not have to be very large to accommodate wide changes in the field. Such a magnetometer should be suitable for use in fields ranging from zero to perhaps 30 or 40 G.

The experimental techniques described herein are possibly capable of use with other alkali atoms having small hyperfine splittings; e.g., K^{41}, Na^{23}, and Rb^{85}. Consideration is being given to the further extension of this work to coherence "carryover" experiments,[27] and combined Zeeman and hyperfine light-beat experiments.

[26] A. L. Bloom, J. Appl. Opt. 1, 61 (1962).
[27] R. B. Partridge and G. W. Series, Proc. Phys. Soc. (London) 88, 969 (1966).